JOURNAL OF VIROLOGY, June 2010, p. 5719–5729 Vol. 84, No. 11
0022-538X/10/$12.00 doi:10.1128/JVI.00134-10

Inhibition of Xenotropic Murine Leukemia Virus-Related Virus by APOBEC3 Proteins and Antiviral Drugs▽

Tobias Paprotka,[1] Narasimhan J. Venkatachari,[1] Chawaree Chaipan,[1] Ryan Burdick,[1] Krista A. Delviks-Frankenberry,[1] Wei-Shau Hu,[2] and Vinay K. Pathak[1]*

Viral Mutation Section,[1] and Viral Recombination Section,[2] HIV Drug Resistance Program, National Cancer Institute at Frederick, Frederick, Maryland 21702

Received 20 January 2010/Accepted 11 March 2010

Xenotropic murine leukemia virus-related virus (XMRV), a gammaretrovirus, has been isolated from human prostate cancer tissue and from activated CD4$^+$ T cells and B cells of patients with chronic fatigue syndrome, suggesting an association between XMRV infection and these two diseases. Since APOBEC3G (A3G) and APOBEC3F (A3F), which are potent inhibitors of murine leukemia virus and Vif-deficient human immunodeficiency virus type 1 (HIV-1), are expressed in human CD4$^+$ T cells and B cells, we sought to determine how XMRV evades suppression of replication by APOBEC3 proteins. We found that expression of A3G, A3F, or murine A3 in virus-producing cells resulted in their virion incorporation, inhibition of XMRV replication, and G-to-A hypermutation of the viral DNA with all three APOBEC3 proteins. Quantitation of A3G and A3F mRNAs indicated that, compared to the human T-cell lines CEM and H9, prostate cell lines LNCaP and DU145 exhibited 50% lower A3F mRNA levels, whereas A3G expression in 22Rv1, LNCaP, and DU145 cells was nearly undetectable. XMRV proviral genomes in LNCaP and DU145 cells were hypermutated at low frequency with mutation patterns consistent with A3F activity. XMRV proviral genomes were extensively hypermutated upon replication in A3G/A3F-positive T cells (CEM and H9), but not in A3G/A3F-negative cells (CEM-SS). We also observed that XMRV replication was susceptible to the nucleoside reverse transcriptase (RT) inhibitors zidovudine (AZT) and tenofovir and the integrase inhibitor raltegravir. In summary, the establishment of XMRV infection in patients may be dependent on infection of A3G/A3F-deficient cells, and cells expressing low levels of A3G/A3F, such as prostate cancer cells, may be ideal producers of infectious XMRV. Furthermore, the anti-HIV-1 drugs AZT, tenofovir, and raltegravir may be useful for treatment of XMRV infection.

Gammaretroviruses infect a wide range of species and are associated with a variety of neurological and immunological disorders, as well as carcinomas and leukemias (9, 11, 21, 30, 58). In 2006, for the first time, a gammaretrovirus was isolated from human tissues and was named xenotropic murine leukemia virus-related virus (XMRV) (63). The virus was discovered to be prevalent in prostate cancer tissues derived from patients carrying a mutation in the *RNASEL* gene, an important player in the interferon-mediated suppression of viral infection in host target cells (48, 53, 54). A recent study found XMRV in several prostate cancer samples with the same prevalence for patients with and without the RNASEL mutation and suggested that XMRV infection may be associated with nearly 30% of all prostate cancers (51). However, two other studies could not confirm an association of XMRV with prostate cancer in Germany, suggesting that XMRV's geographic distribution may not extend to Europe (10, 17). In addition to prostate cancers, XMRV was also recently isolated from chronic fatigue syndrome (CFS) patients, exhibiting a high prevalence of 67% in confirmed cases and a prevalence of 4% in healthy controls (31). However, three other studies failed to find an association between XMRV and CFS (8, 12, 64). The reported high prevalence of XMRV in the general population (4%) also has not been confirmed by independent publications. At this time, it is not clear whether XMRV contributes to the development of prostate cancer and chronic fatigue syndrome, and perhaps other cancers and chronic diseases.

Studies of human immunodeficiency virus type 1 (HIV-1) replication and its interactions with host proteins have revealed the existence of several intracellular defense mechanisms that inhibit the replication of a variety of viral pathogens, including retroviruses (39, 50, 52, 61). The APOBEC3 family of genes encode cytidine deaminases, which provide a potent defense against infections with retroviruses. In humans, APOBEC3G (A3G) and APOBEC3F (A3F) are the most potent inhibitors of HIV-1. A3G and A3F are counteracted by the HIV-1-encoded Vif protein in virus-producing cells, which targets them for proteasomal degradation and suppresses their incorporation into virions (35, 59, 62, 68). During reverse transcription in the infected target cells, A3G and A3F deaminate the cytidines in the viral minus-strand DNA to uridines, resulting in massive G-to-A hypermutation of the viral genome. In addition, A3G and A3F also inhibit viral-DNA synthesis and integration of the viral DNA into the host chromosome (2, 32, 36, 40). APOBEC proteins have been identified in numerous animal species; interestingly, murine APOBEC3 (mA3) is also a potent inhibitor of Vif-deficient HIV-1 (14, 33, 45).

Since human APOBEC3 proteins have also been shown to be potent inhibitors of murine gammaretroviruses, like Moloney murine leukemia virus (MLV) and the endogenous AKV murine leukemia virus, an MLV-like virus derived from AKR mice (6, 27, 45), we sought to determine whether and how A3G

* Corresponding author. Mailing address: HIV Drug Resistance Program, National Cancer Institute-Frederick, P.O. Box B, Building 535, Room 334, Frederick, MD 21702-1201. Phone: (301) 846-1710. Fax: (301) 846-6013. E-mail: vinay.pathak@nih.gov.

▽ Published ahead of print on 24 March 2010.

and A3F inhibit the replication of XMRV. Our results show that XMRV replication is highly sensitive to inhibition by A3G and A3F; furthermore, XMRV proviral genomes were extensively hypermutated in the presence of A3G, A3F, and mA3 and when passaged in T-cell lines expressing A3G and A3F. Since the expression of A3G is undetectable in prostate cancer cell lines, our results suggest that one important parameter for establishing XMRV infection in humans is infection of cells expressing low levels of A3G and A3F, such as prostate cancer cells. Furthermore, we analyzed the abilities of several anti-HIV-1 drugs to inhibit XMRV replication and found that two reverse transcriptase (RT) inhibitors and an integrase inhibitor may be useful for treatment of XMRV replication.

MATERIALS AND METHODS

Plasmids. The XMRV infectious molecular clone VP62 has been previously described (7). MSCV-IRES-Luc is a murine leukemia virus-based vector (Addgene) that expresses the firefly luciferase reporter gene. FLAG-A3G and A3F-FLAG plasmids were previously described (46). The plasmid expressing murine APOBEC3, pc-Mu-APOBEC3G-HA from Nathaniel Landau (34), was obtained through the AIDS Research and Reference Reagent Program, Division of AIDS, NIAID, NIH, and pcDNA 3.1 (−) was obtained from Invitrogen.

Cell culture. Prostate carcinoma cell lines (22Rv1, LNCaP, and DU145) were obtained from the American Type Culture Collection. CEM, CEM-SS, H9, 22Rv1, and LNCaP cells were maintained at 5% CO_2 in RPMI 1640 (CellGro) supplemented with 10% fetal calf serum (FCS) (HyClone) and penicillin/streptomycin (50 U/ml and 50 μg/ml, respectively; Gibco). Human 293T and DU145 cells were maintained at 5% CO_2 in Dulbecco's modified Eagle's medium (DMEM) (CellGro) supplemented with 10% FCS (HyClone) and penicillin/streptomycin (50 U/ml and 50 μg/ml, respectively; Gibco).

Virus production. Human 293T cells were seeded at 4×10^6 cells per 100-mm-diameter dish, and 24 h later, the cells were transfected with 7 μg of VP62 and different concentrations of FLAG-A3G, A3F-FLAG, or mA3-HA expression plasmid. For the luciferase assays, 7 μg of MSCV-IRES-Luc was included in the transfection mixture. pcDNA3.1 (−) without a multiple cloning site was used as a vector control and to maintain equivalent amounts of DNA for each transfection. Polyethyleneimine (PEI) (Sigma) was used for transfection as described previously (46). The virus-containing supernatant was collected 48 h after transfection and filtered through a 0.45-μm filter.

Single-replication-cycle assay. The virus-containing culture supernatants were collected from transfected 293T cells and used to infect LNCaP cells in triplicate in the presence of Polybrene (50 μg/ml) for 4 h. The virus was washed off the LNCaP cells, and the cells were maintained for an additional 48 h. The luciferase activity in LNCaP cell lysates was assayed using the BriteLite Plus ultra-high-sensitivity luminescence reporter gene assay system (Perkin-Elmer) according to the manufacturer's protocol. Luciferase activity was determined by using a 96-well luminometer (Lumistar Galaxy; BMG Labtech).

For testing drug susceptibility in the single-replication-cycle assay, LNCaP cells were plated at a density of 1×10^4 cells per well in a 96-well plate and used as target cells for infection. The reporter viruses were diluted 5- and 50-fold and used to infect target LNCaP cells. The target cells were incubated with media containing serial dilutions of a drug for 6 h before infection, during infection, and after infection. Infection was monitored using the luciferase activity assay as described above. Data were plotted as the percentage inhibition of luciferase activity versus a $\log_{10}$ drug concentration, and the percentage of inhibition was calculated as follows: [1 − (luciferase activity in the presence of drug/luciferase activity in the absence of drug)] × 100%. Inhibition curves defined by the four-parameter sigmoidal function $y = y_0 + a/[1+(x/x_0)^b]$ were fitted to the data by SIGMAPLOT 8.0 software to calculate the drug concentration required to inhibit virus replication by 50% (IC_{50}), as described previously (41).

Western blot analysis. For Western blot analysis of viral proteins, 293T cells were transfected with VP62 and other plasmids; 48 h after transfection, the culture supernatant was filtered through a 0.45-μm filter and concentrated by ultracentrifugation (25,000 rpm for 90 min; Sorvall TH-641 rotor). The 293T cells were washed twice with phosphate-buffered saline and lysed in 1 ml of lysis buffer (50 mM Tris-HCl [pH 7.4] with 150 mM NaCl, 1 mM EDTA, and 1% Triton X-100) containing protease inhibitor cocktail (Roche) by incubation with gentle agitation for 10 min. The cellular debris was removed by centrifugation at 10,000 × *g* for 10 min (46). The virus pellet and the cell lysates were analyzed by loading equal amounts of protein on 4 to 20% polyacrylamide gels and transferred to polyvinylidene difluoride (PVDF) membranes. The flag-tagged A3G and A3F proteins were detected using a rabbit anti-FLAG polyclonal antibody (Bio-Rad) at a 1:10,000 dilution; the hemagglutinin (HA)-tagged mA3 protein was detected using a mouse anti-HA monoclonal antibody (Sigma) at a 1:5,000 dilution. A3G expression was detected using an antibody that was obtained through the AIDS Research and Reference Reagent Program, Division of AIDS, NIAID, NIH—anti-ApoC17 from Klaus Strebel (23) at a 1:5,000 dilution—and the secondary horseradish peroxidase-labeled goat anti-rabbit antibody was obtained from Bio-Rad. The XMRV capsid protein was detected using a cross-reacting monoclonal anti-MLV CA (α-MLV CA) antibody (28) at a 1:200 dilution. As a control for the amount of total protein in cell lysates, α-tubulin was detected using mouse anti-tubulin antibody (Sigma) at a 1:10,000 dilution. The mouse primary antibodies were detected with horseradish peroxidase-labeled goat anti-mouse secondary antibody (Sigma), and the proteins were visualized using the Western Lighting Chemiluminescence Reagent Plus kit (Perkin-Elmer).

Cloning of XMRV proviral DNA from 22Rv1 cells. Total DNA from 22Rv1 cells was isolated using the DNeasy kit (Qiagen), and the XMRV proviral genomic DNA was amplified using two primer pairs. Nucleotides (nt) 56 to 3753 were amplified using a primer covering nucleotides 1 to 55 of the VP62 (DQ399707) sequence and a reverse primer from nt 3682 to 3754 as previously described (7). Nucleotides 3755 to 8117 were amplified with a primer from 3682 to 3754 and a reverse primer with the sequence of nt 8118 to 8185 of VP62. PCR was accomplished with Phusion polymerase (NEB) and purified with AmpureXP (Beckman-Coulter). The amplified DNA fragments were cloned into pcrBLUNT (Invitrogen) and sequenced.

Quantitative real-time RT-PCR assays. Viral RNA was extracted from cell-free supernatant using the QIAamp vRNA minikit (Qiagen) according to the manufacturer's directions. Cellular RNA was extracted from 1×10^6 cells with the RNeasy kit (Qiagen). The extracts were treated with DNase I for 30 min using the Turbo DNA-free kit (Ambion) to avoid any DNA contamination. XMRV RNA was detected by using the quantitative real-time RT-PCR assay. The LightCycler 480 RNA Master Hydrolysis Probes reaction mixture (Roche) was used; the forward and reverse primers (XMRV4552F and XMRV4673R) and probe (XMRV4572MGB) were described previously (51). A3G/A3F were detected with TaqMan gene expression assays (Applied Biosystems) using Hs00222415_m1 for A3G and Hs00736570_m1 for A3F and normalized to porphobilinogen deaminase (PBGD) as described previously (38). Serial 10-fold dilutions of linearized plasmid (VP62, FLAG-A3G, or A3F-FLAG) were used to generate a standard curve. The template RNA was tested for DNA contamination using the LightCycler 480 DNA Probes Master reaction mixture (Roche).

Infection of human cell lines. Confluent 22Rv1 cells were diluted 1:5 and grown for 5 days. The supernatant was harvested, passed through a 0.45-μM filter, and frozen at −80°C. For the adherent prostate cell lines LNCaP and DU145, 1×10^5 cells were seeded in 6-well plates 1 day prior to infection. For the suspension cell lines CEM, CEM-SS, and H9, 1×10^6 cells were seeded into 8-cm^2 flasks. The cells were incubated for 5 h with 100 μl 22Rv1 cell culture supernatant. After incubation, 2 ml medium was added to the cell cultures with adherent cells and 5 ml to the suspension cultures. CEM, CEM-SS, H9, and DU145 cells were diluted 1:3 every 2 days; LNCaP cells were diluted 1:3 every 4 days; and all cultures were harvested at day 16. Prior to infection, all cell lines were analyzed by PCR and tested negative for the presence of XMRV or MLV. As determined by real-time PCR, 100 μl of 22Rv1 supernatant contained about 5.5×10^8 copies of XMRV RNA.

Analysis of G-to-A hypermutation. Total DNA was extracted from cells with DNeasy (Qiagen). DNA extracts of XMRV VP62 plasmid and A3G, A3F, mA3, or vector control cotransfections were treated with DpnI (8 possible sites) prior to the PCR to avoid plasmid contamination. Approximately 1.2 kb of the XMRV genome (nt 2465 to 3660) was amplified with primer XMRV-A-for (5′-TCACC CACTCTTTCCTCCATGTACC-3′) and XMRV-A-rev (5′-GAGTTCAAAGG GCTTAGTCAAATCTGG-3′) using PCR high-fidelity supermix (Invitrogen). PCR fragments were cloned into the pGEM-T Easy vector (Promega) and sequenced with M13 forward and reverse primers.

Nucleotide sequence accession number. The XMRV 22Rv1 consensus sequence has been deposited in GenBank under accession number FN692043.

RESULTS

APOBEC3 proteins inhibit XMRV infection and are incorporated into XMRV virions. APOBEC3 proteins have been shown to inhibit infection of murine gammaretroviruses (6, 27,

45), but their effects on XMRV replication have not been previously determined. To evaluate the effects of human A3G, human A3F, and mA3 proteins on XMRV infectivity, a single-replication-cycle assay was designed (Fig. 1A). Human 293T cells were cotransfected with VP62, an infectious XMRV molecular clone, and MSCV-IRES-Luc reporter plasmid, along with different amounts of A3G, A3F, or mA3 expression plasmid. The infectivity of XMRV and MSCV-IRES-Luc reporter viruses produced in the presence or absence of APOBEC3 proteins was evaluated by infection of LNCaP cells followed by standard luciferase assay. MSCV-IRES-Luc without any VP62 DNA was included as a control to confirm that the luciferase activity measured in the infected LNCaP cells was dependent on the production of infectious XMRV (data not shown). The amount of A3G expressed in cells transfected with 1 μg of FLAG-A3G is comparable to the physiological levels of A3G in producer cells and would incorporate ~7 molecules of A3G per Vif-deficient HIV-1 particle (67). The results from three independent experiments showed that the infectivity of the XRMV and MSCV-IRES-Luc reporter virus produced in the presence of 0.5, 1.0, or 2.0 μg of A3G protein was less than 1% of that observed when the virus was produced in the absence of any APOBEC3 expression plasmid (set to 100%) (Fig. 1B). In the presence of 1, 2, and 4 μg of A3F expression plasmid, the infectivity of the virus was reduced to 20, 9, and 7% of that of the control, respectively, in a dose-dependent manner. Transfection with equivalent amounts of A3G and A3F expression plasmids resulted in less potent inhibition of HIV-1 with A3F than with A3G (18, 37, 47). The reporter virus produced in the presence of 1 μg of mA3 expression vector did not show any reduction in luciferase activity. Increasing the concentration of the mA3 expression vector to 2 and 4 μg reduced the infectivity of the reporter virus to 51% and 37% of that of the control, respectively. These results showed that A3G and A3F proteins are more effective at inhibiting XMRV infectivity than the mA3 protein.

To confirm that the differences seen in the infectivity of the reporter virus produced in the presence of APOBEC3 proteins were not due to differences in the amounts of virus, the cell lysates and the virus from the transfected cells were evaluated by Western blot analysis (Fig. 1C). The results showed that there was no significant difference in the amount of virus produced from the cells as evaluated by α-MLV CA antibody compared to the MLV Gag expression in the cells. As expected, the cell lysates had more unprocessed Gag, whereas most of the Gag in the XMRV virion particles was processed to the mature p30 capsid. The ability of XMRV to package APOBEC3 proteins was evaluated by Western blot analysis. An α-FLAG antibody was used to detect A3G and A3F proteins and an α-HA antibody to detect mA3 protein. The results clearly showed that there was a dose-dependent increase in the incorporation of A3G, A3F, and mA3 proteins in the XMRV virions. Similar results were obtained in three independent experiments.

To rule out the possibility that APOBEC3 proteins were packaged only in virions that packaged MSCV-luc RNA, we transfected XMRV DNA in the presence or absence of APOBEC3 expression plasmids, and the XMRVs produced were used to infect LNCaP cells (Fig. 1D). The proviral DNAs from the infected LNCap cells were amplified by PCR, cloned, and analyzed by sequencing them for the presence of G-to-A hypermutations. The results showed that 2 of 11, 5 of 22, and 6 of 21 proviral DNA clones derived from virus produced in the presence of A3G, A3F, and mA3, respectively, exhibited G-to-A hypermutations (Fig. 1E). Furthermore, most of the G-to-A mutations (67/77, or 87%) in the proviral clones derived from virus produced in the presence of A3G occurred in the GG dinucleotide context, as expected for A3G-mediated cytidine deamination (Fig. 1F). As expected for A3F and mA3 cytidine deamination activity, most of the G-to-A mutations in the proviral clones produced occurred in the GA dinucleotide context (A3F, 89%; mA3, 80%). Together, these results showed that the APOBEC3 proteins can be incorporated into XMRV virions, induce G-to-A hypermutation, and inhibit the infectivity of XMRV.

Rare hypermutation of XMRV proviruses in 22Rv1 cells. It was previously shown that the prostate cancer cell line 22Rv1 (55) produces high levels of infectious XMRV (24). Furthermore, characterization of proviral DNA in 22Rv1 indicated that there are at least 10 proviral-DNA copies in the majority of the 22Rv1 cells. To characterize the proviral DNAs in 22Rv1 cells, we PCR amplified two fragments of XMRV proviral DNA that encoded most of the viral genome, and 20 clones of each PCR product were sequenced. The individual sequences were compared to the XMRV 22Rv1 consensus sequence in order to identify sequence variations. Most of the sequences were identical to the consensus sequence; however, one clone of the 5′ fragment (clone 1.1) and 2 clones of the 3′ fragment (clone 2.1 and 2.2) showed several G-to-A changes relative to the consensus, strongly suggesting hypermutation by APOBEC3 (Fig. 2A). Most of the G-to-A changes occurred in GA dinucleotides (82% [18/22]), 81% [10/12], and 71% [5/7] for clones 1.1, 2.1, and 2.2, respectively (Fig. 2B), suggesting that A3F or another APOBEC3 protein with a similar mutational specificity (A3B or A3H) was responsible for these hypermutation events. Comparing the 22Rv1 consensus sequence to the currently available XMRV full-length sequences (31, 63) indicated only few single-nucleotide mutations (<10), and no hypermutation was found (data not shown).

Expression of A3G and A3F in human prostate cancer and T-cell lines. Human A3G and A3F are expressed in several primary cells, including $CD4^+$ T cells, B cells, and macrophages (26, 42, 60). To determine whether A3G is expressed in human prostate cancer cell lines, we performed quantitative real-time RT-PCR and determined the relative A3G and A3F mRNA levels in the prostate cancer and T-cell lines (Fig. 3A). The results showed that, compared to CEM cells, H9 cells expressed similar levels of A3G mRNA, whereas the permissive CEM-SS T-cell line and all prostate cancer cell lines expressed little or no A3G mRNA. The A3F mRNA levels in the CEM and H9 cells were also similar; however, the permissive CEM-SS cell line and the 22Rv1 cell line expressed little or no A3F mRNA. In addition, the LNCaP and DU145 cells expressed A3F mRNA at about 50% of the levels observed in CEM and H9 cells.

Western blotting was performed using an anti-A3G antiserum, and the levels of A3G in 22Rv1, LNCaP, and DU145 cells were compared to the A3G expression in T-cell lines (Fig. 3B). The results showed that A3G protein was not detectable in any of the prostate cancer cell lines. As expected, A3G

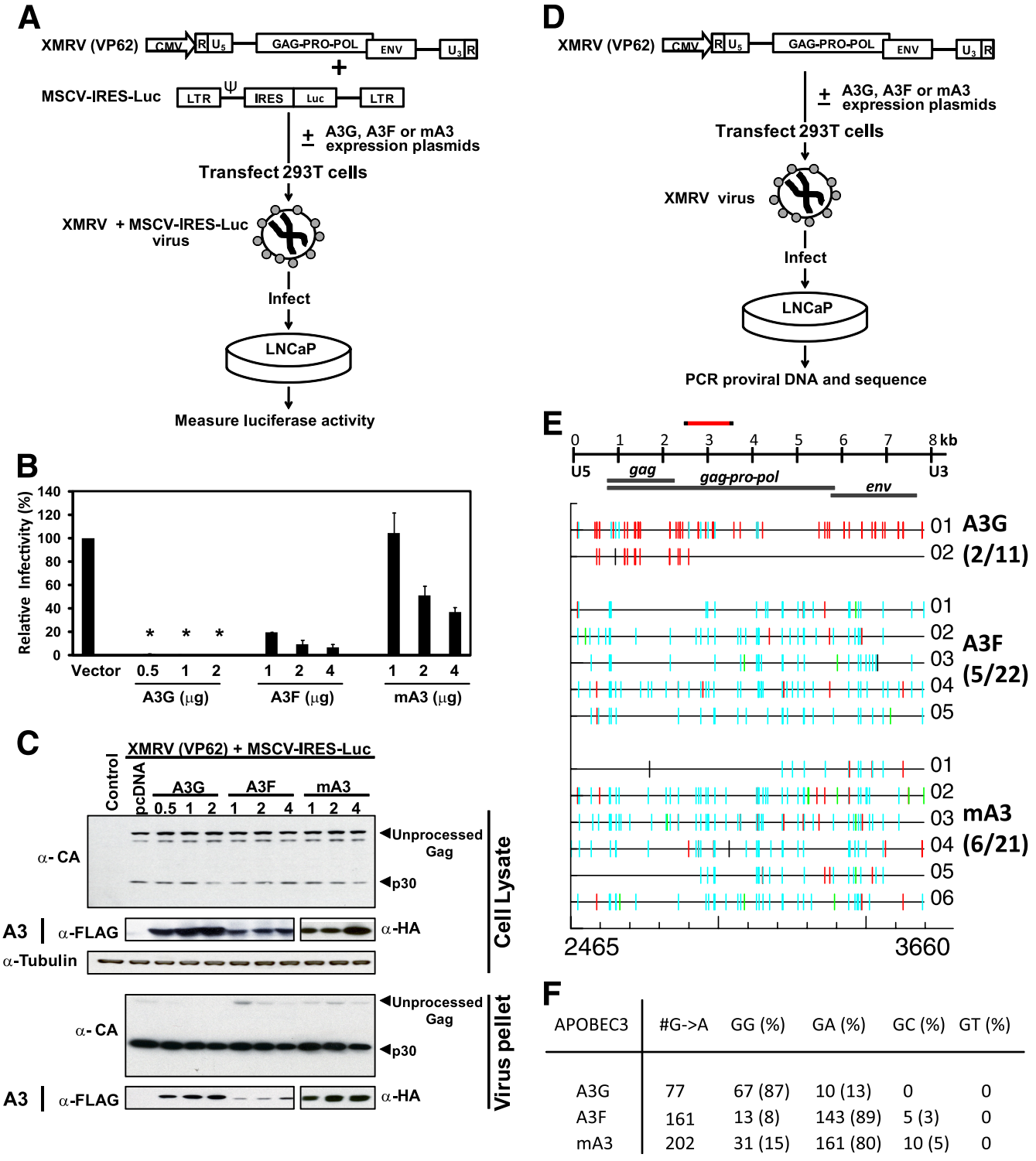

FIG. 1. Effects of A3G, A3F, and mA3 proteins on XMRV infection in single-replication-cycle assay. (A and D) Schematic outline of the experimental design, along with the proviral plasmids used in the experiment. XMRV was produced upon transfection of XMRV infectious molecular clone VP62 with (A) and without (D) MSCV-IRES-Luc reporter plasmids, in the presence or absence of A3G, A3F, or mA3 in 293T cells. The viruses produced were used to infect LNCaP prostate carcinoma cells, and the relative infectivity of the virus was measured by determining firefly luciferase activity in infected cells (A) or by PCR amplifying and sequencing the proviral DNA (D). CMV, cytomegalovirus promoter; R, repeat; U_5, unique 5′; GAG-PRO-POL, GAG-protease-polymerase polyprotein gene; ENV, envelope gene; U_3, unique 3′; LTF, long terminal repeat; Ψ, packaging signal; IRES, internal ribosomal entry site; Luc, luciferase gene. (B) VP62, the MSCV-IRES-Luc plasmid, and different amounts of A3G, A3F, and mA3 expression plasmids were transfected in 293T cells; 48 h posttransfection, the viruses were used to infect LNCaP cells in triplicate. The infected LNCaP cells were lysed 48 h posttransfection, and the luciferase activity in the cell lysates was determined. The luciferase activity in the vector control was set to 100%. The asterisks indicate that luciferase activity was less than 1% of that of the vector

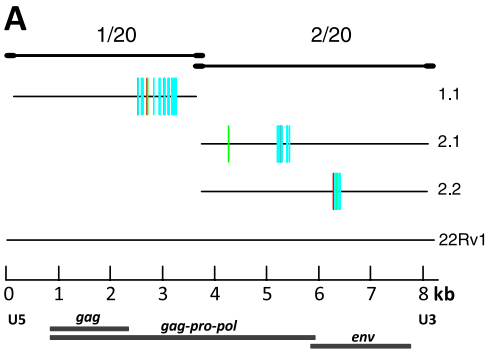

B

Clone	#G->A	GG	GA	GC	GT
1.1	22	3	18	1	0
2.1	12	1	10	1	0
2.2	7	1	5	1	0

FIG. 2. Rare hypermutation in the XMRV 22Rv1 provirus. (A) Mutations in proportion to the XMRV genome that were found while sequencing XMRV-22Rv1. In total, 20 clones each of fragments 1 and 2 were sequenced completely. One clone of fragment 1 (clone 1.1) and 2 clones of fragment 2 (clones 2.1 and 2.2) were found to be hypermutated. The Hypermut color code is described in the legend to Fig. 1. (B) The total number and the sequence context of mutations are shown for each clone. Most of the mutations occurred in the GA dinucleotide context.

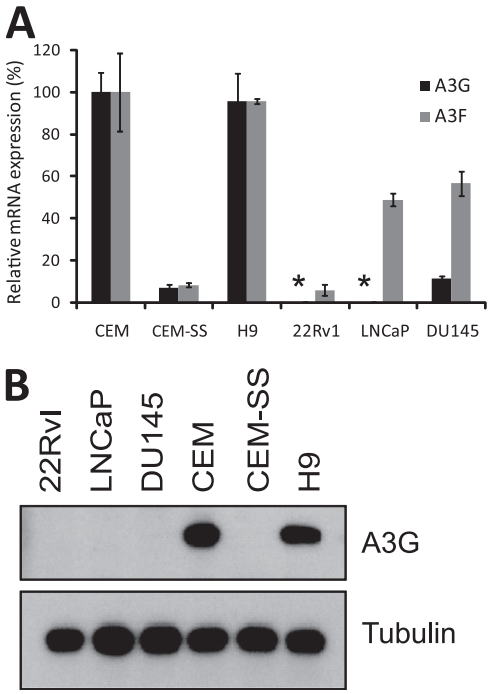

FIG. 3. A3G and A3F mRNA levels and A3G protein expression in prostate cancer and T-cell lines. (A) The A3G and A3F mRNA copy numbers were determined by real-time RT-PCR assays and normalized to PBGD. The reactions were prepared in duplicate, and the average and standard error of 3 independent extractions are shown. Copy numbers below the detection limit of 100 copies are marked with asterisks. (B) Equal amounts of protein (5 μg) from the prostate cancer cell lines 22Rv1, LNCaP, and DU145 and the human T-cell lines CEM, CEM-SS, and H9 were analyzed by Western blotting to detect A3G and α-tubulin, which served as a loading control.

expression was detected in CEM and H9 cells, but not CEM-SS cells. Although we could readily detect A3F protein expression in transfected 293T cells, we were unable to detect A3F protein expression in the prostate cancer or T-cell lines (data not shown).

G-to-A hypermutation of XMRV proviral DNA in human prostate cancer and T-cell lines. To determine whether XMRV DNA is targeted by endogenous levels of APOBEC3 proteins expressed in prostate cancer and T-cell lines, we infected CEM-SS, CEM, H9, LNCaP, and DU145 cells with virus produced from 22Rv1 cells. Proviral DNAs were isolated from the infected cells 16 days after infection, and the ~1.2-kb fragment from the pol region of XMRV proviral DNA was amplified (Fig. 1E). The PCR products were cloned, and their DNA sequences were compared to the 22Rv1 consensus sequence. Analysis of 24 clones obtained from 22Rv1 cells did not reveal any proviral DNAs with hypermutation (Fig. 4A). In total, 14 mutations were observed for 28,680 sequenced nucleotides (mutation frequency, 4.9×10^{-4}/nt). The result indicated that hypermutated proviruses are rare among the proviral DNAs present in 22Rv1 cells. Analysis of 22 clones from infected LNCaP cells revealed a single clone that exhibited several G-to-A mutations (Fig. 4B), indicating that hypermutation of the XMRV proviral genome can occasionally occur in LNCaP cells (35 total mutations for 26,290 nt sequenced; mutation frequency, 1.3×10^{-3}/nt). Similar analysis of infected DU145 cells indicated a higher level of hypermutation, and 5 of 18 clones were hypermutated (Fig. 4C) (126 mutations/21,510 nt sequenced; mutation frequency, 5.6×10^{-3}/nt). The

control. The error bars show the standard deviations of the luciferase activity observed in three independent experiments. (C) Western blot analysis of the incorporation of A3G, A3F, or mA3 protein in XMRV virions. Virus particles were produced in 293T cells by transient transfection of VP62 and MSCV-IRES-Luc in the presence of either 0.5, 1, or 2 μg of A3G expression plasmid; 1, 2, or 4 μg of either A3F or mA3 expression plasmid; or 4 μg of an empty-vector plasmid. The viruses from the supernatant were collected 48 h posttransfection, filtered, and concentrated by ultracentrifugation. At the same time point, the transfected cells were lysed. Equal amounts of cell lysate and equal volumes of concentrated virus were analyzed by immunoblotting them with anti-MLV capsid, anti-FLAG, or anti-HA antibodies. To ensure that equivalent aliquots were loaded onto the gels, the same lysates were analyzed using anti-tubulin antibody. (E) The extent of G-to-A hypermutation was analyzed in the presence of 0.5 μg A3G, 1 μg A3F, and 4 μg mA3. A schematic overview of the XMRV genome is shown, and the region sequenced (nt 2465 to 3660) is indicated with a red bar. The Hypermut (http://www.hir.lanl.gov/content/sequence/HYPERMUT/hypermut.html) color code was used to indicate the mutations: GG to AG in red, GA to AA in cyan, GC to AC in green, GT to AT in magenta, gaps in yellow, and all other mutations in black. In total, 2 of 11 clones were hypermutated in the presence of A3G, 5 of 22 with A3F, and 6 of 21 with mA3. (F) Total numbers of mutations and their occurrence in different dinucleotide contexts. The numbers in parentheses indicate percentages of total G-to-A mutations.

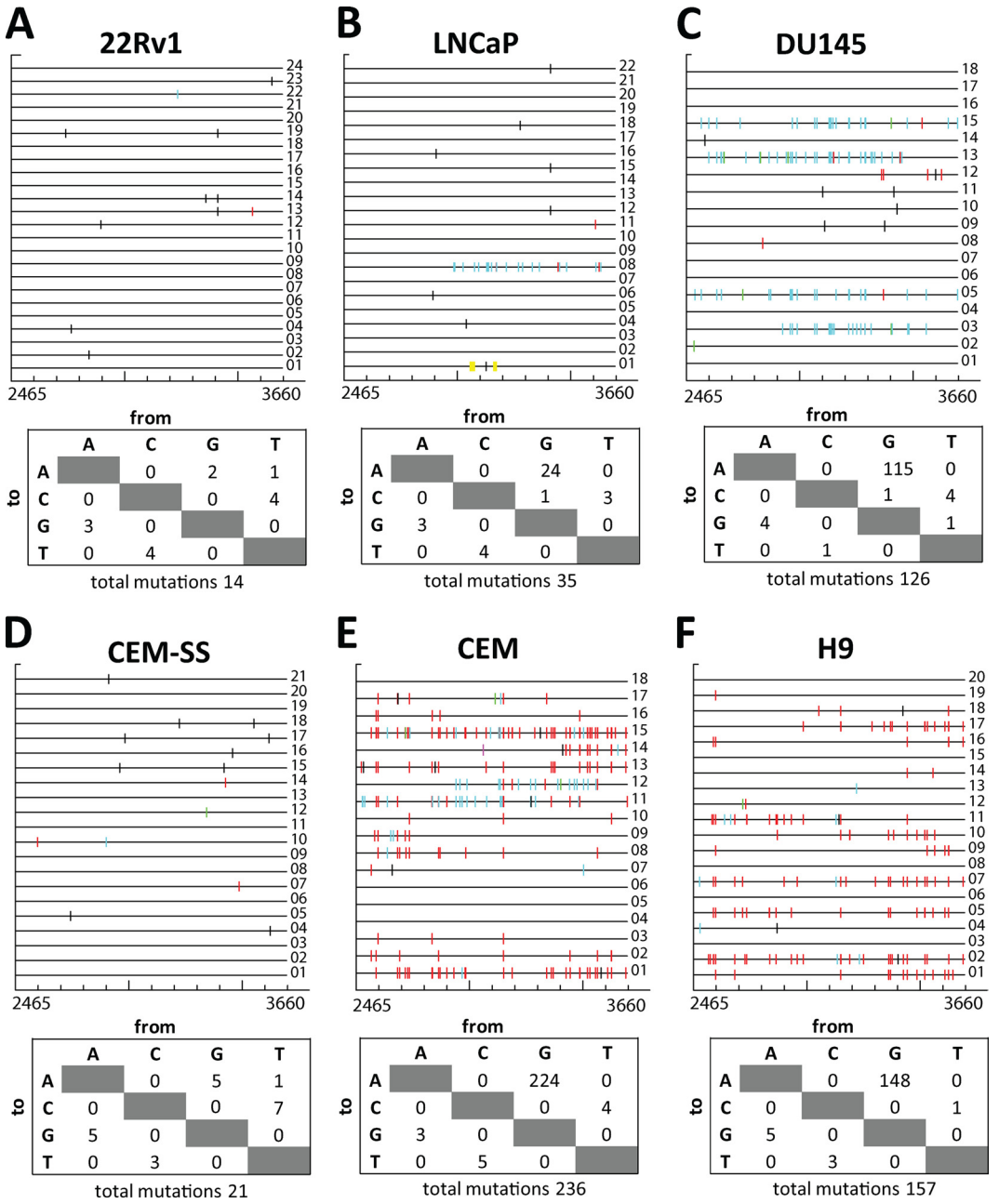

FIG. 4. XMRV hypermutation in prostate cancer and T-cell lines. Mutations found in 22Rv1 (A), LNCaP (B), DU145 (C), CEM-SS (D), CEM (E), and H9 (F) cells in comparison to the XMRV-22Rv1 consensus sequence are marked with vertical bars at their positions. The Hypermut color code is described in the legend to Fig. 1. Below each set of sequences, a detailed table with the total numbers of single-nucleotide mutations is shown.

G-to-A hypermutions in the LNCaP and DU145 cells primarily occurred in the GA dinucleotide context, consistent with A3F activity, and produced stop codons in all hypermutated proviruses.

In the proviral DNAs derived from the human T-cell line CEM-SS, which does not express significant levels of A3G or A3F mRNA, no G-to-A hypermutation was detected (Fig. 4D). A total of 21 mutations were detected in 25,095 nucleotides sequenced, and the mutation frequency (8.4×10^{-4}/nt) was similar to that in 22Rv1 proviral DNA.

In contrast to the results obtained from prostate cancer cell lines and CEM-SS cells, a majority of the proviral-DNA clones obtained from CEM and H9 cells, which express A3G protein, were extensively hypermutated (Fig. 4E and F, respectively). Fourteen of 18 proviral-DNA clones obtained from CEM cells and 13 of 20 clones obtained from H9 cells were hypermutated. The overall mutation frequencies of 1.1×10^{-2}/nt for CEM cells (236 mutations for 21,510 nucleotides sequenced) and 6.6×10^{-3}/nt (157 mutations for 23,900 nucleotides sequenced) were at least 10-fold higher than the mutation fre-

TABLE 1. Dinucleotide context of G-to-A mutations

Cell line	No. of sequences	Dinucleotide context of G-to-A mutations[a]				
		GG	GA	GC	GT	Total
22Rv1	24	1 (50)	1 (50)	0	0	2 (0)
CEM-SS	21	3 (60)	1 (20)	1 (20)	0	5 (0)
CEM	18	171 (76.5)	48 (21.5)	3 (1.5)	1 (0.5)	223 (4.2)
DU145	18	11 (10)	97 (84)	7 (6)	0	115 (2.2)
H9	20	138 (93)	9 (6)	1 (1)	0	148 (2.5)
LNCaP	22	4 (17)	20 (83)	0	0	24 (0.4)

[a] The percentage of mutated G nucleotides (percentage of all analyzed G nucleotides for totals) is shown in parentheses.

quency observed in CEM-SS cells. The mutations found were primarily G-to-A substitutions in the GG dinucleotide context, indicative of a mutational specificity characteristic of A3G (Table 1). The frequency of G-to-A changes in the GA dinucleotide context was also significantly increased, suggesting cytidine deamination and hypermutation by A3F. In addition to causing several changes in the protein amino acid sequence, stop codons were produced in 11 of the hypermutated sequences from CEM cells and 12 from H9 cells. Quantitative real-time RT-PCR analysis showed that the viral-RNA copy numbers in the culture supernatants of CEM, H9, and CEM-SS cells were within 10-fold of each other (8×10^5 to 8×10^6/ml; data not shown). Similar levels of virus production in the presence or absence of A3G/A3F expression may have been due to initial infection at a high multiplicity of infection. In summary, XMRV DNA was targeted by human APOBEC3 proteins in CEM and H9 cells and was extensively hypermutated, leading to amino acid changes and generation of stop codons.

XMRV is sensitive to HIV-1 RT and IN inhibitors. Several anti-HIV-1 drugs were screened for the ability to inhibit XMRV replication and to possibly provide a drug treatment for XMRV infection. Drugs normally used to target the HIV-1 RT and integrase enzymes were tested for the ability to also block XMRV infection in a single-cycle replication assay. The HIV-1 luciferase reporter virus pseudotyped with vesicular stomatitis virus envelope protein (VSV-G) and the XMRV and MSCV-IRES-luciferase reporter virus were used to infect target LNCaP cells pretreated with various concentrations of each drug to determine the IC_{50}s.

Comparison of the RT inhibitors zidovudine (AZT), lamivudine (3TC), didanosine (ddI), stavudine (d4T), abacavir (ABC), tenofovir (TDF), and the phosphonic acid derivative foscarnet showed only AZT and TDF to be effective at blocking XMRV replication at concentrations similar to those that inhibited HIV-1. As shown in Fig. 5, the susceptibility of XMRV to AZT (0.045 ± 0.007 μM) was similar to that of HIV-1 (0.03 ± 0.014 μM). In the case of 3TC, XMRV was about 10-fold more resistant to 3TC (36.9 ± 5.2 μM) than HIV-1 (3.4 ± 1.4 μM). This was also true for ddI (110 ± 62.4 μM), d4T (9.0 ± 4.2 μM), and ABC (14.4 ± 0.45 μM). The IC_{50} of TDF for XMRV was 3.9-fold higher than that for HIV-1 (1.48 ± 1.05 μM versus 0.38 ± 0.13 μM, respectively), and foscarnet failed to inhibit XMRV infection even at a concentration of 250 μM. The HIV-1 integrase inhibitor raltegravir was able to inhibit XMRV at nanomolar concentrations (0.82 ± 0.07 nM), with XMRV being 2.5-fold more susceptible than HIV-1 (2.25 ± 0.21 nM). Overall, these results suggest that AZT, TDF, and raltegravir can effectively inhibit XMRV infection at concentrations that are similar to those needed to inhibit HIV-1 infection, whereas substantially higher doses of 3TC, ddI, d4T, and ABC are required to inhibit XMRV infection.

DISCUSSION

Recent reports of XMRV infection in humans (31, 51, 63) have raised important questions as to how XMRV evades the natural human immune responses, including the intracellular defense provided by the APOBEC3 proteins. Identification of prostate cancer cells that were defective for the *RNASEL* gene (mutation R462Q) provided some evidence that XMRV was likely replicating in humans by evading the interferon-induced 2-5A/RNASEL pathway; however, in other studies, having a defective *RNASEL* gene was not associated with XMRV infection in prostate cancer or CFS patients (31, 51).

The APOBEC3 family of cytidine deaminase proteins restricts exogenous retroviruses and endogenous retroelements by several mechanisms, including G-to-A hypermutation, inhibition of DNA synthesis, and provirus formation (3, 15, 19, 36). Our studies show for the first time that XMRV is susceptible to human APOBEC3 proteins. We found a strong restriction of XMRV by A3G and A3F, suggesting that efficient spread of XMRV from cells expressing high levels of these proteins is unlikely. It is therefore noteworthy that XMRV infection and replication in human $CD4^+$ T cells, B cells, and activated peripheral blood mononuclear cells (PBMCs) was recently reported (31). All of these cells have been shown to express APOBEC3 proteins (26); furthermore, in the case of activated PBMCs and $CD4^+$ T cells, A3G/A3F expression has been associated with potent inhibition of Vif-deficient HIV-1 (5, 65). Despite potent inhibition, it remains possible that a small proportion of XMRVs can escape APOBEC3-mediated inhibition, allowing low levels of viral replication to persist even in cells that express APOBEC3 proteins. It would be of interest to verify that XRMV replication occurs in these primary human cells and to determine the mechanism by which XMRV might evade A3G/A3F-mediated inhibition.

We observed a low frequency of hypermutated proviral clones in LNCaP cells (1 of 22) and DU145 cells (5 of 18). These hypermutations were in the GA dinucleotide context, which is consistent with A3F cytidine deaminase activity. Since LNCaP and DU145 cells have been shown to support XMRV replication (7, 57), it appears that the A3F mRNA levels and the low level of hypermutation in these cell lines are not sufficient to prevent the replication and spread of XMRV. Recent studies have suggested that there are differences between the levels of viral replication in the two cell lines; the reasons for these differences are not clear and may be related to the viral long terminal repeat (LTR) promoter activity (43). The levels of A3G/A3F expression in normal and cancerous prostate tissues are not known, and it would be of interest to determine whether these levels differ from those in the prostate cancer cell lines analyzed here.

XMRV's sensitivity to human APOBEC3 proteins suggests

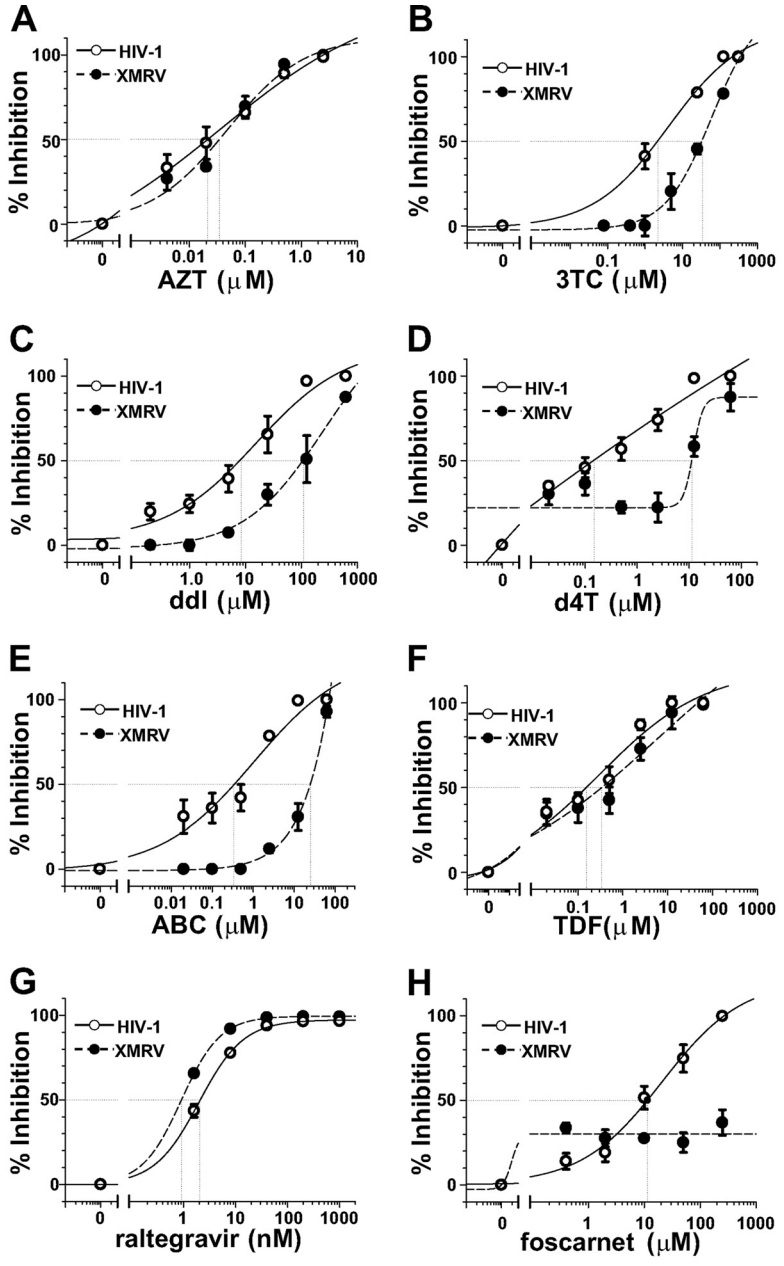

I

	HIV-1 (IC_{50} ± SD)	XMRV (IC_{50} ± SD)
AZT (μM)	0.03 ± 0.014	0.045 ± 0.007
3TC (μM)	3.38 ± 1.39	36.85 ± 5.16
ddI (μM)	13.43 ± 5.6	110.1 ± 62.44
d4T (μM)	0.51 ± .27	9.00 ± 4.23
ABC (μM)	1.01 ± 0.26	14.42 ± 0.45
TDF (μM)	0.38 ± 0.13	1.48 ± 1.05
raltegravir (nM)	2.25 ± 0.21	0.82 ± 0.07
foscarnet (μM)	9.58 ± 1.99	> 250

FIG. 5. Single-replication-cycle drug susceptibility assays. Phenotypic drug susceptibility testing for AZT (A), 3TC (B), ddI (C), d4T (D), ABC (E), TDF (F), raltegravir (G), and foscarnet (H) was performed with HIV-1 (pNLuc + VSV-G) (open circles) and XMRV (VP62+MSCV-IRES-Luc) (filled circles) reporter viruses in LNCaP cells. The intersections of the vertical lines with the drug concentration axis show the IC_{50} for each curve. Representative graphs are shown. (I) The mean IC_{50}s and standard deviations were calculated using SIGMAPLOT 8.0 as described in Materials and Methods.

that it has not evolved mechanisms to evade these proteins, perhaps because it is a relatively new infection in the human population. Only a few full-length genome sequences from individual patients have been published so far (31, 63), and their low genetic variation supports this hypothesis. It has been observed that A3F is a less potent inhibitor of HIV-1 replication than A3G (18, 47), and we also observed a less potent inhibition of XMRV with A3F than with A3G. However, A3F was expressed at a lower level than A3G in our experiments, and additional studies will be needed to determine whether XMRV replication is more sensitive to A3G than to A3F.

Our results showed that XMRV proviral genomes were extensively hypermutated in CEM and H9 cells, which express A3G, but not in CEM-SS cells, which express little or no A3G (52). These results show that, in addition to a reduction in infectivity, APOBEC3 proteins also cause substantial G-to-A hypermutation of the XMRV genome, leading to truncated or nonfunctional viral proteins. The absence of significant genetic diversity among different XMRVs isolated from different patients, and the apparent absence of hypermutation, supports the view that XMRV replication primarily occurs in cells that do not express or express low levels of APOBEC3 proteins.

As previously shown for MLV and AKV (6, 27, 45), XMRV was also much less sensitive to mA3 than A3G or A3F. This could indicate that XMRV is more adapted to the mouse innate immune response and that transmission to humans occurred recently. Interestingly, our results show that cotransfection with mA3 resulted in hypermutation of XMRV proviral genomes. Recent studies have shown that the AKV proviral genomes, but not MLV proviral genomes, are hypermutated by mA3, even though mA3 is incorporated into both AKV and MLV virions (27). Our results indicate that XMRV's sensitivity to mA3-mediated hypermutation is similar to that of AKV and is unlike the resistance to hypermutation exhibited by MLV.

The mechanism involved in XMRV's and MLV's reduced sensitivity to mA3 restriction is currently unknown. Some studies hypothesized that MLV may exclude mA3 from virions as a way to avoid hypermutation and maintain a productive infection, while others report mA3 encapsidation without inhibition of viral replication (6, 25, 27, 34, 45, 69). Our results agree with the latter studies and show that both human and murine APOBEC3 proteins can be incorporated into XMRV virions when expressed in human-derived cell lines.

The prostate carcinoma cell line 22Rv1 (55), which is most likely heterogeneous, contains approximately 10 stably integrated copies of XMRV and expresses high levels of XMRV (24). We sequenced XMRV proviruses from the 22Rv1 cells and found that only 1 of 20 PCR clones obtained from the 5′ half of the genome showed evidence of G-to-A hypermutation, mainly in a GA dinucleotide context (29). Sequencing of an additional 24 PCR products derived from the same region (Fig. 3B) did not identify any additional hypermutated PCR products, suggesting that hypermutated genomes were probably present in only a small subpopulation of the 22Rv1 cells. When virions produced from the 22Rv1 cells were used to infect CEM-SS cells, we did not observe any hypermutation, suggesting little or no expression of A3F. It is not clear how the hypermutated proviruses in the 22Rv1 cells were generated, but transient low-level expression of A3F, or A3F expression in a minor subpopulation of cells, could have resulted in hypermutation of these proviruses.

The results of our studies are in general agreement with those recently reported by Groom et al. (13), who found that XMRV replication is highly sensitive to A3G (200-fold inhibition) and, to a lesser extent, A3B (65- to 80-fold inhibition); they also found that A3A, A3C, A3F, and A3H inhibited XMRV replication by less than 10-fold. The differences in sensitivity to A3F between the two studies may have resulted from differences in the ratios of the A3F and XMRV plasmid DNAs used in the cotransfections or other experimental conditions.

Although it has not been established that XMRV infection contributes to the pathogeneses of prostate cancer and CFS, it is prudent to identify treatments that may be useful in suppressing XMRV replication. We analyzed several antiviral drugs that are currently approved for treatment of HIV-1 infection by the U.S. Food and Drug Administration for their abilities to suppress XMRV infection. We found that AZT inhibited XMRV replication, as recently reported by Sakuma et al. and Hong et al. (20, 49) and consistent with previously reported inhibition of MLV replication (22, 44, 56). We also found that TDF inhibits XMRV replication, albeit with less potency than HIV-1, and that raltegravir, recently reported to inhibit MLV integration (1), is a potent inhibitor of XMRV. These antiviral agents may be useful for analysis of the kinetics of XMRV replication; such studies have provided great insights into the mechanisms of HIV-1 replication and pathogenesis (4, 16, 66). It will also be of interest to determine whether and how XMRV can develop resistance to these inhibitors and to compare the mechanisms of resistance to those observed in HIV-1 replication. Most importantly, it may be possible to devise combination antiviral therapy for treatment of XMRV infection using these inhibitors.

In summary, our results show that XMRV is strongly restricted and hypermutated by human A3G and A3F proteins. Therefore, efficient XMRV replication and spread may require cells that express low levels of these proteins, such as prostate cancer cells. In addition, the HIV-1 RT inhibitors AZT and TDF, as well as the integrase inhibitor raltegravir, may be useful for treatment of XMRV infection.

ACKNOWLEDGMENTS

We especially thank Robert Silverman for providing the XMRV clone VP62 and for insightful discussions during manuscript preparation. We also thank Eric Freed and Alan Rein for valuable discussions during manuscript preparation.

This research was supported in part by the Intramural Research Program of the NIH, National Cancer Institute, Center for Cancer Research.

The content of this publication does not necessarily reflect the views or policies of the Department of Health and Human Services, nor does mention of trade names, commercial products, or organizations imply endorsement by the U.S. Government.

REFERENCES

1. **Beck-Engeser, G. B., D. Eilat, T. Harrer, H. M. Jack, and M. Wabl.** 2009. Early onset of autoimmune disease by the retroviral integrase inhibitor raltegravir. Proc. Natl. Acad. Sci. U. S. A. **106:**20865–20870.
2. **Bishop, K. N., M. Verma, E. Y. Kim, S. M. Wolinsky, and M. H. Malim.** 2008. APOBEC3G inhibits elongation of HIV-1 reverse transcripts. PLoS Pathog. **4:**e1000231.
3. **Chiu, Y. L., and W. C. Greene.** 2008. The APOBEC3 cytidine deaminases: an

innate defensive network opposing exogenous retroviruses and endogenous retroelements. Annu. Rev. Immunol. **26:**317–353.
4. **Coffin, J. M.** 1995. HIV population dynamics in vivo: implications for genetic variation, pathogenesis, and therapy. Science **267:**483–489.
5. **Dang, Y., X. Wang, T. Zhou, I. A. York, and Y. H. Zheng.** 2009. Identification of a novel WXSLVK motif in the N terminus of human immunodeficiency virus and simian immunodeficiency virus Vif that is critical for APOBEC3G and APOBEC3F neutralization. J. Virol. **83:**8544–8552.
6. **Doehle, B. P., A. Schafer, H. L. Wiegand, H. P. Bogerd, and B. R. Cullen.** 2005. Differential sensitivity of murine leukemia virus to APOBEC3-mediated inhibition is governed by virion exclusion. J. Virol. **79:**8201–8207.
7. **Dong, B., S. Kim, S. Hong, J. Das Gupta, K. Malathi, E. A. Klein, D. Ganem, J. L. Derisi, S. A. Chow, and R. H. Silverman.** 2007. An infectious retrovirus susceptible to an IFN antiviral pathway from human prostate tumors. Proc. Natl. Acad. Sci. U. S. A. **104:**1655–1660.
8. **Erlwein, O., S. Kaye, M. O. McClure, J. Weber, G. Wills, D. Collier, S. Wessely, and A. Cleare.** 2010. Failure to detect the novel retrovirus XMRV in chronic fatigue syndrome. PLoS One **5:**e8519.
9. **Fan, H.** 1997. Leukemogenesis by Moloney murine leukemia virus: a multistep process. Trends Microbiol. **5:**74–82.
10. **Fischer, N., O. Hellwinkel, C. Schulz, F. K. Chun, H. Huland, M. Aepfelbacher, and T. Schlomm.** 2008. Prevalence of human gammaretrovirus XMRV in sporadic prostate cancer. J. Clin. Virol. **43:**277–283.
11. **Fujino, Y., K. Ohno, and H. Tsujimoto.** 2008. Molecular pathogenesis of feline leukemia virus-induced malignancies: insertional mutagenesis. Vet. Immunol. Immunopathol. **123:**138–143.
12. **Groom, H. C., V. C. Boucherit, K. Makinson, E. Randal, S. Baptista, S. Hagan, J. W. Gow, F. M. Mattes, J. Breuer, J. R. Kerr, J. P. Stoye, and K. N. Bishop.** 2010. Absence of xenotropic murine leukaemia virus-related virus in UK patients with chronic fatigue syndrome. Retrovirology **7:**10.
13. **Groom, H. C., M. W. Yap, R. P. Galao, S. J. Neil, and K. N. Bishop.** 2010. Susceptibility of xenotropic murine leukemia virus-related virus (XMRV) to retroviral restriction factors. Proc. Natl. Acad. Sci. U. S. A. **107:**5166–5171.
14. **Harris, R. S., K. N. Bishop, A. M. Sheehy, H. M. Craig, S. K. Petersen-Mahrt, I. N. Watt, M. S. Neuberger, and M. H. Malim.** 2003. DNA deamination mediates innate immunity to retroviral infection. Cell **113:**803–809.
15. **Harris, R. S., and M. T. Liddament.** 2004. Retroviral restriction by APOBEC proteins. Nat. Rev. Immunol. **4:**868–877.
16. **Ho, D. D., A. U. Neumann, A. S. Perelson, W. Chen, J. M. Leonard, and M. Markowitz.** 1995. Rapid turnover of plasma virions and CD4 lymphocytes in HIV-1 infection. Nature **373:**123–126.
17. **Hohn, O., H. Krause, P. Barbarotto, L. Niederstadt, N. Beimforde, J. Denner, K. Miller, R. Kurth, and N. Bannert.** 2009. Lack of evidence for xenotropic murine leukemia virus-related virus (XMRV) in German prostate cancer patients. Retrovirology **6:**92.
18. **Holmes, R. K., F. A. Koning, K. N. Bishop, and M. H. Malim.** 2007. APOBEC3F can inhibit the accumulation of HIV-1 reverse transcription products in the absence of hypermutation. Comparisons with APOBEC3G. J. Biol. Chem. **282:**2587–2595.
19. **Holmes, R. K., M. H. Malim, and K. N. Bishop.** 2007. APOBEC-mediated viral restriction: not simply editing? Trends Biochem. Sci. **32:**118–128.
20. **Hong, S., E. A. Klein, J. Das Gupta, K. Hanke, C. J. Weight, C. Nguyen, C. Gaughan, K. A. Kim, N. Bannert, F. Kirchhoff, J. Munch, and R. H. Silverman.** 2009. Fibrils of prostatic acid phosphatase fragments boost infections with XMRV (xenotropic murine leukemia virus-related virus), a human retrovirus associated with prostate cancer. J. Virol. **83:**6995–7003.
21. **Jolicoeur, P.** 1991. Neuronal loss in a lower motor neuron disease induced by a murine retrovirus. Can. J. Neurol. Sci. **18:**411–413.
22. **Julias, J. G., T. Kim, G. Arnold, and V. K. Pathak.** 1997. The antiretrovirus drug 3′-azido-3′-deoxythymidine increases the retrovirus mutation rate. J. Virol. **71:**4254–4263.
23. **Kao, S., E. Miyagi, M. A. Khan, H. Takeuchi, S. Opi, R. Goila-Gaur, and K. Strebel.** 2004. Production of infectious human immunodeficiency virus type 1 does not require depletion of APOBEC3G from virus-producing cells. Retrovirology **1:**27.
24. **Knouf, E. C., M. J. Metzger, P. S. Mitchell, J. D. Arroyo, J. R. Chevillet, M. Tewari, and A. D. Miller.** 2009. Multiple integrated copies and high-level production of the human retrovirus XMRV (xenotropic murine leukemia virus-related virus) from 22Rv1 prostate carcinoma cells. J. Virol. **83:**7353–7356.
25. **Kobayashi, M., A. Takaori-Kondo, K. Shindo, A. Abudu, K. Fukunaga, and T. Uchiyama.** 2004. APOBEC3G targets specific virus species. J. Virol. **78:**8238–8244.
26. **Koning, F. A., E. N. Newman, E. Y. Kim, K. J. Kunstman, S. M. Wolinsky, and M. H. Malim.** 2009. Defining APOBEC3 expression patterns in human tissues and hematopoietic cell subsets. J. Virol. **83:**9474–9485.
27. **Langlois, M. A., K. Kemmerich, C. Rada, and M. S. Neuberger.** 2009. The AKV murine leukemia virus is restricted and hypermutated by mouse APOBEC3. J. Virol. **83:**11550–11559.
28. **Lee, S. K., K. Nagashima, and W. S. Hu.** 2005. Cooperative effect of gag proteins p12 and capsid during early events of murine leukemia virus replication. J. Virol. **79:**4159–4169.
29. **Liddament, M. T., W. L. Brown, A. J. Schumacher, and R. S. Harris.** 2004. APOBEC3F properties and hypermutation preferences indicate activity against HIV-1 in vivo. Curr. Biol. **14:**1385–1391.
30. **Linenberger, M. L., and J. L. Abkowitz.** 1995. Haematological disorders associated with feline retrovirus infections. Baillieres Clin. Haematol. **8:**73–112.
31. **Lombardi, V. C., F. W. Ruscetti, J. Das Gupta, M. A. Pfost, K. S. Hagen, D. L. Peterson, S. K. Ruscetti, R. K. Bagni, C. Petrow-Sadowski, B. Gold, M. Dean, R. H. Silverman, and J. A. Mikovits.** 2009. Detection of an infectious retrovirus, XMRV, in blood cells of patients with chronic fatigue syndrome. Science **326:**585–589.
32. **Luo, K., T. Wang, B. Liu, C. Tian, Z. Xiao, J. Kappes, and X. F. Yu.** 2007. Cytidine deaminases APOBEC3G and APOBEC3F interact with human immunodeficiency virus type 1 integrase and inhibit proviral DNA formation. J. Virol. **81:**7238–7248.
33. **Mangeat, B., P. Turelli, G. Caron, M. Friedli, L. Perrin, and D. Trono.** 2003. Broad antiretroviral defence by human APOBEC3G through lethal editing of nascent reverse transcripts. Nature **424:**99–103.
34. **Mariani, R., D. Chen, B. Schrofelbauer, F. Navarro, R. Konig, B. Bollman, C. Munk, H. Nymark-McMahon, and N. R. Landau.** 2003. Species-specific exclusion of APOBEC3G from HIV-1 virions by Vif. Cell **114:**21–31.
35. **Marin, M., K. M. Rose, S. L. Kozak, and D. Kabat.** 2003. HIV-1 Vif protein binds the editing enzyme APOBEC3G and induces its degradation. Nat. Med. **9:**1398–1403.
36. **Mbisa, J. L., R. Barr, J. A. Thomas, N. Vandegraaff, I. J. Dorweiler, E. S. Svarovskaia, W. L. Brown, L. M. Mansky, R. J. Gorelick, R. S. Harris, A. Engelman, and V. K. Pathak.** 2007. Human immunodeficiency virus type 1 cDNAs produced in the presence of APOBEC3G exhibit defects in plus-strand DNA transfer and integration. J. Virol. **81:**7099–7110.
37. **Mbisa, J. L., W. Bu, and V. K. Pathak.** 2010. APOBEC3F and APOBEC3G inhibit HIV-1 DNA integration by different mechanisms. J. Virol. **84:**5250–5259.
38. **Mbisa, J. L., K. A. Delviks-Frankenberry, J. A. Thomas, R. J. Gorelick, and V. K. Pathak.** 2009. Real-time PCR analysis of HIV-1 replication post-entry events. Methods Mol. Biol. **485:**55–72.
39. **Neil, S. J., T. Zang, and P. D. Bieniasz.** 2008. Tetherin inhibits retrovirus release and is antagonized by HIV-1 Vpu. Nature **451:**425–430.
40. **Newman, E. N., R. K. Holmes, H. M. Craig, K. C. Klein, J. R. Lingappa, M. H. Malim, and A. M. Sheehy.** 2005. Antiviral function of APOBEC3G can be dissociated from cytidine deaminase activity. Curr. Biol. **15:**166–170.
41. **Nikolenko, G. N., K. A. Delviks-Frankenberry, S. Palmer, F. Maldarelli, M. J. Fivash, Jr., J. M. Coffin, and V. K. Pathak.** 2007. Mutations in the connection domain of HIV-1 reverse transcriptase increase 3′-azido-3′-deoxythymidine resistance. Proc. Natl. Acad. Sci. U. S. A. **104:**317–322.
42. **Pido-Lopez, J., T. Whittall, Y. Wang, L. A. Bergmeier, K. Babaahmady, M. Singh, and T. Lehner.** 2007. Stimulation of cell surface CCR5 and CD40 molecules by their ligands or by HSP70 up-regulates APOBEC3G expression in CD4(+) T cells and dendritic cells. J. Immunol. **178:**1671–1679.
43. **Rodriguez, J. J., and S. P. Goff.** 2010. Xenotropic murine leukemia virus-related virus establishes an efficient spreading infection and exhibits enhanced transcriptional activity in prostate carcinoma cells. J. Virol. **84:**2556–2562.
44. **Rosenblum, L. L., G. Patton, A. R. Grigg, A. J. Frater, D. Cain, O. Erlwein, C. L. Hill, J. R. Clarke, and M. O. McClure.** 2001. Differential susceptibility of retroviruses to nucleoside analogues. Antivir. Chem. Chemother. **12:**91–97.
45. **Rulli, S. J., Jr., J. Mirro, S. A. Hill, P. Lloyd, R. J. Gorelick, J. M. Coffin, D. Derse, and A. Rein.** 2008. Interactions of murine APOBEC3 and human APOBEC3G with murine leukemia viruses. J. Virol. **82:**6566–6575.
46. **Russell, R. A., M. D. Moore, W. S. Hu, and V. K. Pathak.** 2009. APOBEC3G induces a hypermutation gradient: purifying selection at multiple steps during HIV-1 replication results in levels of G-to-A mutations that are high in DNA, intermediate in cellular viral RNA, and low in virion RNA. Retrovirology **6:**16.
47. **Russell, R. A., and V. K. Pathak.** 2007. Identification of two distinct human immunodeficiency virus type 1 Vif determinants critical for interactions with human APOBEC3G and APOBEC3F. J. Virol. **81:**8201–8210.
48. **Sadler, A. J., and B. R. Williams.** 2008. Interferon-inducible antiviral effectors. Nat. Rev. Immunol. **8:**559–568.
49. **Sakuma, R., T. Sakuma, S. Ohmine, R. H. Silverman, and Y. Ikeda.** 2010. Xenotropic murine leukemia virus-related virus is susceptible to AZT. Virology **397:**1–6.
50. **Sayah, D. M., E. Sokolskaja, L. Berthoux, and J. Luban.** 2004. Cyclophilin A retrotransposition into TRIM5 explains owl monkey resistance to HIV-1. Nature **430:**569–573.
51. **Schlaberg, R., D. J. Choe, K. R. Brown, H. M. Thaker, and I. R. Singh.** 2009. XMRV is present in malignant prostatic epithelium and is associated with prostate cancer, especially high-grade tumors. Proc. Natl. Acad. Sci. U. S. A. **106:**16351–16356.
52. **Sheehy, A. M., N. C. Gaddis, J. D. Choi, and M. H. Malim.** 2002. Isolation of a human gene that inhibits HIV-1 infection and is suppressed by the viral Vif protein. Nature **418:**646–650.

53. **Silverman, R. H.** 2007. A scientific journey through the 2-5A/RNase L system. Cytokine Growth Factor Rev. **18:**381–388.
54. **Silverman, R. H.** 2007. Viral encounters with 2′,5′-oligoadenylate synthetase and RNase L during the interferon antiviral response. J. Virol. **81:**12720–12729.
55. **Sramkoski, R. M., T. G. Pretlow II, J. M. Giaconia, T. P. Pretlow, S. Schwartz, M. S. Sy, S. R. Marengo, J. S. Rhim, D. Zhang, and J. W. Jacobberger.** 1999. A new human prostate carcinoma cell line, 22Rv1. In Vitro Cell Dev. Biol. Anim. **35:**403–409.
56. **Stair, R. K., C. J. Nelson, and J. W. Mellors.** 1991. Use of recombinant retroviruses to characterize the activity of antiretroviral compounds. J. Virol. **65:**6339–6342.
57. **Stieler, K., C. Schulz, M. Lavanya, M. Aepfelbacher, C. Stocking, and N. Fischer.** 2010. Host range and cellular tropism of the human exogenous gammaretrovirus XMRV. Virology **399:**23–30.
58. **Stocking, C., and C. A. Kozak.** 2008. Murine endogenous retroviruses. Cell Mol. Life Sci. **65:**3383–3398.
59. **Stopak, K., C. de Noronha, W. Yonemoto, and W. C. Greene.** 2003. HIV-1 Vif blocks the antiviral activity of APOBEC3G by impairing both its translation and intracellular stability. Mol. Cell **12:**591–601.
60. **Stopak, K. S., Y. L. Chiu, J. Kropp, R. M. Grant, and W. C. Greene.** 2007. Distinct patterns of cytokine regulation of APOBEC3G expression and activity in primary lymphocytes, macrophages, and dendritic cells. J. Biol. Chem. **282:**3539–3546.
61. **Stremlau, M., C. M. Owens, M. J. Perron, M. Kiessling, P. Autissier, and J. Sodroski.** 2004. The cytoplasmic body component TRIM5alpha restricts HIV-1 infection in Old World monkeys. Nature **427:**848–853.
62. **Svarovskaia, E. S., H. Xu, J. L. Mbisa, R. Barr, R. J. Gorelick, A. Ono, E. O. Freed, W. S. Hu, and V. K. Pathak.** 2004. Human apolipoprotein B mRNA-editing enzyme-catalytic polypeptide-like 3G (APOBEC3G) is incorporated into HIV-1 virions through interactions with viral and nonviral RNAs. J. Biol. Chem. **279:**35822–35828.
63. **Urisman, A., R. J. Molinaro, N. Fischer, S. J. Plummer, G. Casey, E. A. Klein, K. Malathi, C. Magi-Galluzzi, R. R. Tubbs, D. Ganem, R. H. Silverman, and J. L. DeRisi.** 2006. Identification of a novel Gammaretrovirus in prostate tumors of patients homozygous for R462Q RNASEL variant. PLoS Pathog. **2:**e25.
64. **van Kuppeveld, F. J., A. S. Jong, K. H. Lanke, G. W. Verhaegh, W. J. Melchers, C. M. Swanink, G. Bleijenberg, M. G. Netea, J. M. Galama, and J. W. van der Meer.** 2010. Prevalence of xenotropic murine leukaemia virus-related virus in patients with chronic fatigue syndrome in the Netherlands: retrospective analysis of samples from an established cohort. BMJ **340:**c1018.
65. **Vetter, M. L., M. E. Johnson, A. K. Antons, D. Unutmaz, and R. T. D'Aquila.** 2009. Differences in APOBEC3G expression in CD4+ T helper lymphocyte subtypes modulate HIV-1 infectivity. PLoS Pathog. **5:**e1000292.
66. **Wei, X., S. K. Ghosh, M. E. Taylor, V. A. Johnson, E. A. Emini, P. Deutsch, J. D. Lifson, S. Bonhoeffer, M. A. Nowak, B. H. Hahn, et al.** 1995. Viral dynamics in human immunodeficiency virus type 1 infection. Nature **373:**117–122.
67. **Xu, H., E. Chertova, J. Chen, D. E. Ott, J. D. Roser, W. S. Hu, and V. K. Pathak.** 2007. Stoichiometry of the antiviral protein APOBEC3G in HIV-1 virions. Virology **360:**247–256.
68. **Yu, X., Y. Yu, B. Liu, K. Luo, W. Kong, P. Mao, and X. F. Yu.** 2003. Induction of APOBEC3G ubiquitination and degradation by an HIV-1 Vif-Cul5-SCF complex. Science **302:**1056–1060.
69. **Zhang, L., X. Li, J. Ma, L. Yu, J. Jiang, and S. Cen.** 2008. The incorporation of APOBEC3 proteins into murine leukemia viruses. Virology **378:**69–78.